

# MMM 2022 Conference

Minneapolis, MN • October 31 - November 4, 2022 • [www.magnetism.org](http://www.magnetism.org)

## BOOK OF ABSTRACTS

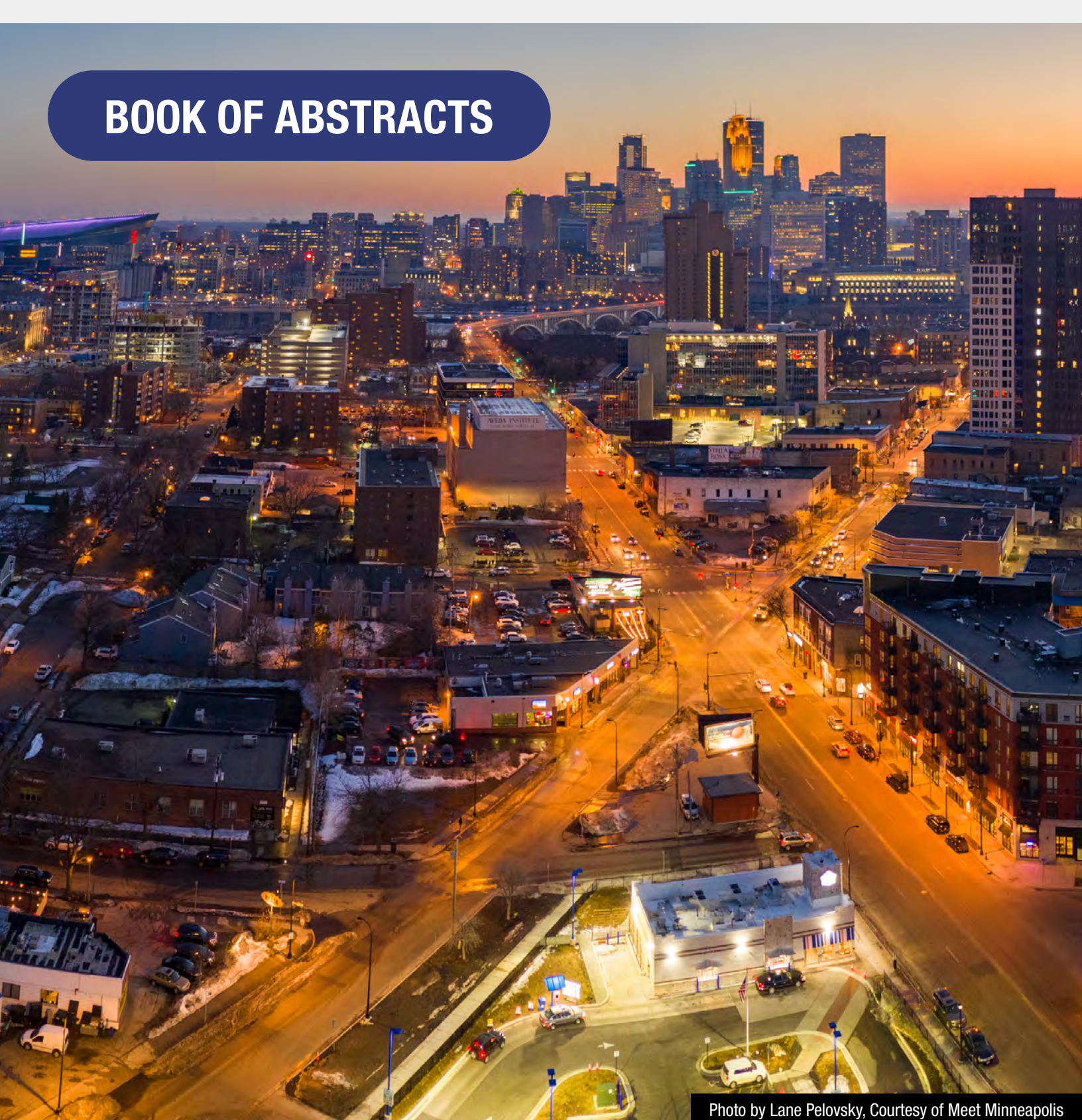


Photo by Lane Pelovsky, Courtesy of Meet Minneapolis

**Session NPB**  
**MAGNETOCALORIC MATERIALS III**  
**(Poster Session)**

Arjun Pathak, Chair

State University of New York, Buffalo State, Buffalo, NY, United States

**NPB-01. The change of atomic environments caused by Co doping in La(Fe<sub>1-x</sub>Co<sub>x</sub>)<sub>11.4</sub>Si<sub>1.6</sub> magnetocaloric materials.** *B. Wang<sup>1</sup>, H. Zhou<sup>1</sup>, F. Hu<sup>1</sup> and B. Shen<sup>1</sup>. 1. Institute of Physics, Chinese Academy of Sciences, Beijing, China*

Solid-state refrigeration based on magnetocaloric effect (MCE) has been regarded as an attractive alternative to the conventional gas compression technique. La(Fe,Si)<sub>13</sub> materials exhibit giant MCE and negative thermal expansion (NTE), which are regarded as one of the most likely materials to be used in room temperature magnetic refrigeration. Our recent study proved that hydrostatic pressure in La(Fe<sub>0.92</sub>Co<sub>0.08</sub>)<sub>11.1</sub>Si<sub>1.1</sub> sharpens the magnetoelastic transition and enlarges the volume change during the transition, through alerting the intra-icosahedron Fe-Fe bonds (B1, B2, B3) rather than the inter-icosahedral bonds (B4, B5) in the NaZn<sub>13</sub>-type structure, thus MCE and barocaloric effect get enhanced. However, Co doping in La(Fe<sub>1-x</sub>Co<sub>x</sub>)<sub>11.4</sub>Si<sub>1.6</sub> induces the decrease of MCE, where the intrinsic mechanism remains unknown. In order to clarify the essence from atom level, we studied the doping-dependent variation of Fe-Fe bonds by Co in La(Fe<sub>1-x</sub>Co<sub>x</sub>)<sub>11.4</sub>Si<sub>1.6</sub> ( $x=0, 0.06$ ) by variable temperature XRD and Rietveld refinements. Unlike hydrostatic pressure, due to Co doping, the five Fe-Fe bonds have different elongations in the temperature range 150~300K covering phase transition (Fig.2). This demonstrates the increase in exchange distance and enhancement of the exchange interaction, which is consistent with a large increase in the Curie temperature (Fig.1a). Compared to LaFe<sub>11.4</sub>Si<sub>1.6</sub> with negative volume change  $\Delta V/V$  (-1.30%) during FM-PM transition, La(Fe<sub>0.94</sub>Co<sub>0.06</sub>)<sub>11.4</sub>Si<sub>1.6</sub> shows a decreased  $\Delta V/V$  (-0.96%) by 26.2% in magnitude and the phase transition becomes slower (Fig.1b). Similar study on doping at La sites is under way. Examining the variation of atom local environments can provide insight for understanding the intrinsic origin of magnetocaloric properties, which is helpful for optimizing magnetocaloric materials.

[1] Shen B., Sun J., Hu F., et al. *Adv. Mater.*, 21, 4545 (2009). [2] Hu F., Shen B., Sun J., et al. *Appl. Phys. Lett.*, 78, 3675 (2001). [3] Fujita A., Fujieda S., Fukamichi K. *Phys. Rev. B*, 65, 014410 (2001). [4] Wang G., Wang F., Di N., et al. *J. Magn. Magn. Mater.*, 303, 84 (2006). [5] Gschneidner K. A., Mudryk Y., Pecharsky V. K. *Scr. Mater.*, 67, 572 (2012). [6] Hao J., Hu F., Wang J., et al. *Chem. Mater.*, 32, 1807 (2020).

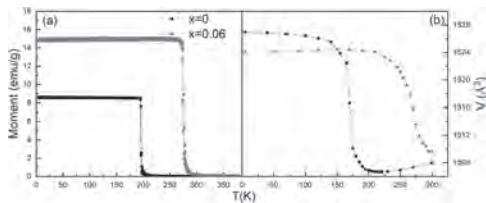


**Fig.1 (a)** M-T curves under 0.01T and **(b)** lattice volume as a function of temperature for La(Fe<sub>1-x</sub>Co<sub>x</sub>)<sub>11.4</sub>Si<sub>1.6</sub>.

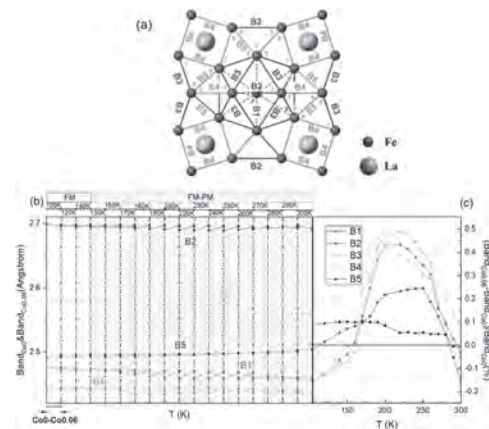


**Fig. 2** (a) Schematic view of Fe-Fe bonds in LaFe<sub>13</sub> with NaZn<sub>13</sub>-type structure, (b) the compared Fe-Fe bonds for La(Fe<sub>1-x</sub>Co<sub>x</sub>)<sub>11.4</sub>Si<sub>1.6</sub> with and without 6 at.% Co doping at different temperatures covering phase transition temperature, (c) the change ratio of Fe-Fe bonds caused by 6 at.% Co doping.

**NPB-02. The effect of acid treatment on the magnetic and magnetocaloric properties of Al-rich Al<sub>0.85+x</sub>Si<sub>0.15</sub>Fe<sub>2</sub>B<sub>2</sub>.** *K.M. Stillwell<sup>1</sup>, B. Birch<sup>1</sup>, N. Kramer<sup>3</sup>, B. Reese<sup>1</sup>, A. Pathak<sup>2</sup> and M. Khan<sup>1</sup>. 1. Physics, Miami University, Oxford, OH, United States; 2. Ames National Laboratory, Ames, IA, United States; 3. SUNY Buffalo State College, Buffalo, NY, United States*

Owing to the relative abundance of its constituent elements and large MCE observed near room temperature, the AlFe<sub>2</sub>B<sub>2</sub> system has attracted much attention recently [1]. As an alternative to current rare earth materials, AlFe<sub>2</sub>B<sub>2</sub> promises the realization of cleaner, energy efficient refrigeration technologies based on phenomena associated with MCE [2]. Additionally, excess Al is believed to generate phase impurities which can change the observed MCE properties of this system [3]. By dissolving certain impurities in acid, a significant enhancement of the MCE properties of this system have been observed [4]. Considering this behavior, we have studied the effect of acid treatment on the magnetic, magnetocaloric, and transport properties of Al<sub>0.85+x</sub>Si<sub>0.15</sub>Fe<sub>2</sub>B<sub>2</sub> ( $x = 0.2, 0.4$ ). The goal was to explore the possibility of enhancing the MCE properties of the materials by adding excess aluminum and subjecting them to acid treatment after annealing. The samples were prepared by arc melting followed by drop-casting. The drop-casted samples were annealed followed by acid treatment. The alloys were characterized by x-ray diffraction, scanning electron microscopy, dc magnetization, and electrical resistivity measurements. The second order ferromagnetic phase transitions were observed near room temperature (~298 K – 315 K) and peak magnetic entropy changes ( $-\Delta S_M$ ) of more than 4 J/kg K were observed for a field change of 5 T. The details of phase purity, microstructure, magnetic, and transport properties of the acid treated and the drop casted annealed materials will be presented.

[1] A. Loudaini, M. Aggour, L. Bahmad, O. Mounkachi, Magnetic properties, magnetocaloric effect and cooling performance of AlFe<sub>2</sub>B<sub>2</sub> compound: Ab initio, Monte Carlo and numerical modeling study, Materials Science and Engineering: B, 264 (2021). [2] Xiaoyan Tan, Ping Chai, Corey M.

Thompson, Michael Shatruk, Magnetocaloric Effect in AlFe2B2: Toward Magnetic Refrigerants from Earth-Abundant Elements, Journal of the American Chemical Society, 135 Iss. 25 9553-9557 (2013). [3] Tahir Ali, M. N. Khan, E. Ahmed, Asad Ali, Phase analysis of AlFe2B2 by synchrotron X-ray diffraction, magnetic and Mossbauer studies, Progress in Natural Science: Materials International, 27 251-256 (2017). [4] J.W. Lee, M.S. Song, B.K. Cho, Chunghee Nam, Magnetic properties of pure AlFe2B2 formed through annealing followed by acid-treatment, Curr Appl Phys., 19 933-937 (2019).

**NPB-03. Magnetocaloric properties of Co-doped  $Mn_{0.5}Fe_{0.5}Ni_{1-x}Co_xSi_{0.94}Al_{0.06}$  intermetallic alloys.** S. Bhattacharjee<sup>1</sup>, N. Kramer<sup>2</sup>, M. Khan<sup>1</sup> and A. Pathak<sup>2</sup> 1. Physics, Miami University, Oxford, OH, United States; 2. Physics, State University of New York, Buffalo, NY, United States

Magnetic refrigeration is an environmentally friendly cooling technology, which is believed to be significantly more efficient than the currently employed gas-compression-based cooling technologies. The commercialization of this technology is crucially dependent on the discovery of materials that exhibit large magnetocaloric effects and can be easily fabricated using cheap, non-toxic, and readily available elements. The intermetallic  $Mn_{1-x}Fe_{x-\delta}Ni_{\delta}Si_{1-y}Al_y$  compounds are known to exhibit large magnetocaloric effects at the relatively low magnetic field ( $H = 2$  T or lower) and tunable phase transition [1, 2]. These materials have gained much interest in recent years due to the fact that the constituent elements are cheap and readily available. However, selected drawbacks including large thermal hysteresis and mechanical instability make these materials unsuitable for application. More research efforts are required to eliminate these drawbacks so that the application potential for these materials can be realized. Therefore, we have synthesized the substitution of Ni with Co in  $Mn_{0.5}Fe_{0.5}Ni_{1-x}Co_xSi_{0.94}Al_{0.06}$  ( $0.025 \leq x \leq 0.075$ ) alloys by arc melting followed by a rapidly quenched vacuum suction casting technique and study the magnetic and magnetocaloric properties of the system, which has not been reported yet. X-ray diffraction and scanning electron microscopy (SEM) data indicated that the samples exhibited a single-phase. Peak magnetic entropy changes of ( $-\Delta S_M$ ) of as-cast alloy with  $x = 0.025$  is found to be 12 and 31 J kg<sup>-1</sup>K<sup>-1</sup> for  $\Delta H = 2$  and 5 T, respectively around 225 K. The observed large MCEs are due to the first order magneto-structural phase transition exhibited by the materials from low-temperature ferromagnetic orthorhombic phase to high-temperature paramagnetic hexagonal phase. In this presentation, we present details of phase purity, microstructure, and magnetic properties of as-prepared and heat-treated alloys with  $0.025 \leq x \leq 0.075$

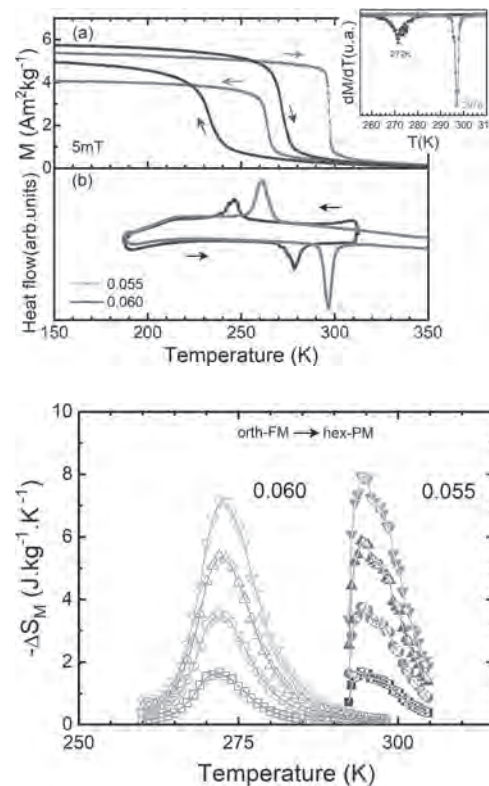
[1] A. Biswas, A.K. Pathak, N.A. Zarkevich, X. Liu, Y. Mudryk, V. Balema, D.D. Johnson, and V.K. Pecharsky, Acta Mater. 180, 341 (2019). [2] M Khan, RC Das, J Casey, BL Reese, B Akintunde, AK Pathak, AIP Advances 12, 035227 (2022).

**NPB-04. Magnetostructural transition and magnetocaloric effect in thermally annealed  $Mn_{0.5}Fe_{0.5}NiSi_{1-x}Al_x$  melt-spun ribbons ( $x = 0.055$  and  $0.060$ ).** M.d. Arreguin Hernandez<sup>2,1</sup>, A. Dzubinska<sup>2</sup>, M. Reiffers<sup>3</sup>, J. Sanchez<sup>1,4</sup>, C.F. Sanchez Valdés<sup>3</sup> and R. Varga<sup>2</sup> 1. Materiales, Instituto Potosino de Investigación Científica y Tecnológica, San Luis Potosí, Mexico; 2. CPM-TIP, UPJS, Kosice, Slovakia; 3. Faculty of Humanities and Natural Sciences, University of Presov, Presov, Slovakia; 4. Departamento de Física, Universidad de Oviedo, Oviedo, Spain; 5. Div. Multidisciplinaria, UACJ, Ciudad Juarez, Mexico

The giant magnetocaloric (MC) effect measured in  $Mn_{0.5}Fe_{0.5}NiSi_{1-x}Al_x$  alloys ( $0.05 \leq x \leq 0.07$ ) for a low magnetic field change ( $|\Delta S_M|^{max} \sim 16-24$  J kg<sup>-1</sup>K<sup>-1</sup> at 2 T) [1], and the fact that they are based on cheap and abundant elements motivated the interest on their study. The effect is linked to their first-order martensitic-like magnetostructural transformation (MST) from a high-temperature hexagonal Ni<sub>2</sub>In-type paramagnetic (PM) phase to a low-temperature orthorhombic TiNiSi-type ferromagnetic (FM) phase which is tunable over wide temperature range by changing the Al content [1,2].

As melt spinning is a rapid solidification technique able to produce alloy ribbon samples with a high chemical homogeneity and may result very appropriate to fabricate these five-elements alloys, we produced  $Mn_{0.5}Fe_{0.5}NiSi_{1-x}Al_x$  melt-spun ribbons with  $x=0.055$  and 0.060 that were thermally annealed at 1123 K for 4 h; their MST and MC characteristics were studied. RT XRD patterns show that samples are nearly single phase with a major Ni<sub>2</sub>In-type phase coexisting with a minor amount of the TiNiSi-type one. DSC,  $M(T)^{5mT}$  and  $M(T)^{2T}$  curves, shown in Fig. 1, denote the occurrence of the MST with a large thermal hysteresis (~ 32 K), the substantial effect of Al-content on the tuning of the MST temperature without a significant change in the magnetization change across the MST which led to similar  $\frac{1}{2}\Delta S_M(T)|_{T^{max}}$  values (as Fig. 2 shows). The results are discussed and compared with previous data reported in literature for bulk alloys.

[1] A. Biswas et al., Acta Mater. 180, 341–348 (2019). [2] C.L. Zhang et al., Appl. Phys. Lett. 105, 242403 (2014).

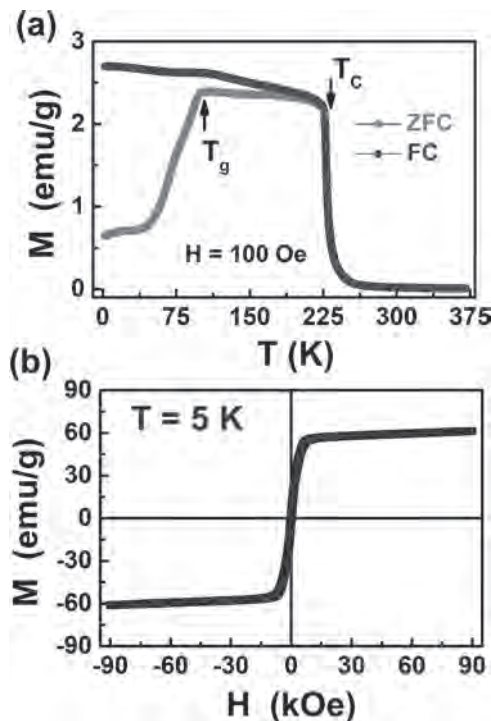


**NPB-05. Magnetocaloric properties and exchange bias in arc melted  $Mn_5Sn_3$  alloy.** L. Bachhraj<sup>1</sup>, P. Babu<sup>2</sup> and G. Basheed<sup>1</sup> 1. CSIR-National Physical Laboratory, New Delhi, India; 2. UGC-DAE Consortium for Scientific Research, Mumbai Centre, BARC Campus, Mumbai, India

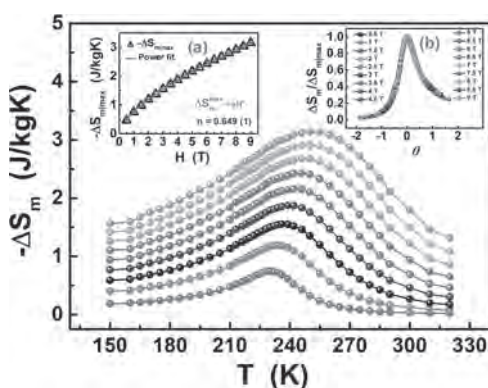
Magnetic refrigeration (MR), exploiting the adiabatic demagnetization phenomena, is preferable over conventional cooling technology due to its high efficiency with environment friendly method [1-3]. Owing to this, the earth-abundant Mn-based alloys, i.e.  $Mn_5Sn_3$ , crystallizes in Ni<sub>2</sub>In type hexagonal structure (space group  $P6_3/mmc$ ), occupies two non-equivalently sites with opposite spin alignment: Mn<sub>I</sub> at 2a site with a moment of 0.8  $\mu_B$  and Mn<sub>II</sub> at 2(d) site with a moment of 3.8  $\mu_B$  and Sn atom occupies 2c site. The temperature and field-dependent dc magnetization measurements have been carried out to study the MCE and exchange bias in  $Mn_5Sn_3$  alloy. The M (T) curve at 100 Oe shows ordering temperature at  $T_c \sim 227$  K and spin glass (SG) transition at  $T_g \sim 110$  K [Fig. 1a]. The origin of SG is due to geometrical frustration, that comes from vacancy and disordering present at Mn<sub>2d</sub> site. Furthermore, the M (H) hysteresis loop at 5 K reveals the typical soft ferromagnetic behaviour, saturation magnetisation ( $M_S$ ) of 62 emu/g [Fig.1(b)], where MH loop slightly shifted towards a negative field direction,

indicating the presence of exchange bias phenomena with exchange bias field ( $H_{EB}$ ) 5.67 mT at 50 K. Apart from this, Isothermal magnetic entropy change ( $\Delta S_M(T)$ ) is (calculated Using Maxwell equation) 2.16 J/Kg-K at 5 T [Fig. 2], also  $\Delta S_M(T)$  evolve with applied magnetic field as -  $\Delta S_M(T) = aH^n$ , where n is local exponent, power law fit gives  $n = 0.649$  (1) [Inset of Fig 2(a)]. From Inset fig. 2(b), It is quite apparent that all the normalized entropy curves with various  $\Delta H$  values collapse into a single curve, confirming second-order magnetic phase transition. The relative cooling power (RCP) value is obtained as 242 J/kg for a field change of 5 T which is significantly larger than the earlier reported  $Mn_3Sn_3$  study [4]. Hence, with negligible thermal/magnetic hysteresis and reasonable RCP, the  $Mn_3Sn_3$  is prominent candidate for MR devices.

1. V. Franco, J. Bluez, J. Ipus, J. Law, L. Moreno - Ramz, A. Conde, Prog. Mater. Sci. 93, (2018) 112–232. 2. V. K. Pecharsky, K. A. Gschneidner Jr, J. Magn. Magn. Mater. 200 (1), (1999) 44–56. 3. V. Franco, J. Blazquez, B. Ingale, A. Conde, Annu. Rev. Mater. Res. 42, (2012) 305–342. 4. Jian Huang, Jie Xiang, Ce Zhi, Xuezhen Wang, Xueling Hou, Adv. Mat. Res. 299-300 (2011) 520-524.



(a) MT curve of  $Mn_3Sn_3$  alloy under 100 Oe applied magnetic field, (b) MH loop measured at 5 K upto 9 T.



The temperature dependence of  $-\Delta S_m$  in the field range of 1 T – 9 T ( $\Delta H = 1$  T), Inset (a): Power-law behaviour of  $-\Delta S_m|_{max}$ , (b): Normalized  $-\Delta S_m$  as a function of the rescaled temperature ( $\theta$ )

#### NPB-06. Large reversible magnetocaloric effects in $Pr_{2-x}Nd_xIn$ .

A. Biswas<sup>1</sup>, R.K. Chouhan<sup>1</sup>, A. Thayer<sup>1,2</sup>, Y. Mudryk<sup>1</sup>, O. Dolotko<sup>1</sup> and V. Pecharsky<sup>1,2</sup> 1. Ames National Laboratory, Ames, IA, United States; 2. Department of Materials Science and Engineering, Iowa State University, Ames, IA, United States

Over the last few decades, interest in discovery of materials that exhibit large magnetocaloric effects below room temperature and can support energy-efficient magnetocaloric liquefaction of various gases is on the rise. Here we report a series of rare-earth based  $Pr_{2-x}Nd_xIn$  compounds, where Curie temperatures are tunable by adjusting  $x_{Nd}$  between 57 and 110 K. Every member of the family exhibits a sharp magnetic transition between the paramagnetic and ferromagnetic states. These transitions give rise to magnetic field-induced entropy changes comparable to or larger than those reported in any other known material in the same temperature range, making  $Pr_{2-x}Nd_xIn$  compounds suitable for liquefaction of technologically important gases including oxygen, nitrogen, and natural gas. The magnetic transitions in these intermetallics do not show any detectable thermomagnetic hysteresis which is advantageous from the application point of view. While the transition temperature increases with  $x_{Nd}$ , the maximum entropy change is slightly reduced from 15 J/Kg K at 57 K when  $x_{Nd} = 0$  to 13 J/Kg K at 110 K when  $x_{Nd} = 2$ , all quoted values are for the magnetic field changing between 0 and 2 T. Notably, the thermodynamic nature of phase transitions for the end-members of the series is different. In case of  $Pr_2In$ , the transition is first-order magnetoelastic, as evidenced by symmetry-invariant discontinuous changes in cell volume occurring in concert with the ferromagnetic ordering/disordering transitions.<sup>1,2</sup> Conversely, the phase transition in  $Nd_2In$  is rather unconventional, being intermediate between a typical first-order and a typical second-order kind. Density functional theory calculations, providing insights into the electronic structure of the end members and expounding differences in their physical behaviors, will be also discussed. Acknowledgement: This work was performed at Ames National Laboratory (AMES) and was supported by the Division of Materials Science and Engineering of the Office of Basic Energy Sciences of the U.S. Department of Energy (DOE). AMES is operated for the U.S DOE by Iowa State University under Contract No. DE-AC02-07CH11358.

1. A. Biswas, R. K. Chouhan, O. Dolotko, A. Thayer, S. Lapidus, Y. Mudryk, V. K. Pecharsky, ECS J. Solid State Sci. Technol. 11, 043005 (2022). 2. A. Biswas, N. A. Zarkevich, A. K. Pathak, O. Dolotko, I. Z. Hlova, Y. Mudryk, D. D. Johnson, V. K. Pecharsky, Phys. Rev. B 101, 224402 (2020).

#### NPB-07. Effect of X-Ray Irradiation on Magnetocaloric Material, $(MnNiSi)_{1-x}(Fe_2Ge)_x$ .

J.J. Nunez<sup>1</sup>, V. Sharma<sup>1</sup>, J. Rojas<sup>1</sup>, R. Barua<sup>1</sup> and R.L. Hadimani<sup>1,2</sup> 1. Mechanical & Nuclear Engineering, Virginia Commonwealth University, Richmond, VA, United States; 2. Psychiatry, Harvard University, Boston, MA, United States

Magnetic refrigeration based on magnetocaloric effect at room temperature is generally considered a potential substitution for classical vapor compression systems due to its high efficiency and environmental friendliness.  $(MnNiSi)_{1-x}(Fe_2Ge)_x$  materials are attractive multicaloric materials that change their magnetic properties with the application of magnetic field, pressure, and temperature [1],[2]. The effects of electron and proton irradiation techniques in magnetocaloric materials have been reported in peer-reviewed articles therefore, this study investigated the effects of X-ray irradiation on  $(MnNiSi)_{1-x}(Fe_2Ge)_x$ . Polycrystalline  $(MnNiSi)_{1-x}(Fe_2Ge)_x$  samples were prepared by arc-melting the constituent elements of purity better than 99.9% in an ultrahigh argon atmosphere to ensure sample homogeneity[2]. The procedure utilized X-RAD 225XL Precision X-Ray. The study evidences an observable effect in the  $(MnNiSi)_{1-x}(Fe_2Ge)_x$ ,  $x = 0.34$  composition when exposed to an absorbed X-ray dosage of ~120Gy/min for 5 hours. A Quantum Design PPMS was used to measure the magnetization (M) of the  $(MnNiSi)_{1-x}(Fe_2Ge)_x$  with applied magnetic fields from -3T to 3T. Fig.1(a) shows the M-T data from 200K to 350K with  $T_c \sim 292$ K before treatment and 286K after treatment (cooling curve). There was also a significant change in the magnetization ~47.4% from 2.72 emu/g to 4.01 emu/g at an applied magnetic field=100Oe. Fig.1(b) presents the M-H (magnetization vs.

magnetic field) loops from 300K to 345K as it exhibited irradiation-induced hysteresis in comparison to the pristine sample. Fig.2(a) exhibits an observable change of 10Oe in the magnetic coercivity at 200K after treatment. Fig.2(b) presents the hysteresis graphs for the samples at 200K and shows a saturation magnetization decrease but yielded an increase in magnetization from H=0Oe-4500Oe for the treated sample. These presented results would provide base guidelines for factors affecting the performance of magnetocaloric materials in extreme environments.

[1] Zhang, C. L., et al. "Magnetostructural Transition and Magnetocaloric Effect in MnNiSi-Fe<sub>2</sub>Ge System." *Applied Physics Letters*, vol. 107, no. 21, 2015, p. 212403., <https://doi.org/10.1063/1.4936610>. [2] D. Clifford, V. Sharma, K. Deepak, R. V. Ramanujan, and R. Barua, "Multicaloric Effects in (MnNiSi)<sub>1-x</sub>(Fe<sub>2</sub>Ge)<sub>x</sub> Alloys," in *IEEE Transactions on Magnetics*, vol. 57, no. 2, pp. 1-5, Feb. 2021, Art no. 2500405, doi: 10.1109/TMAG.2020.3025002.

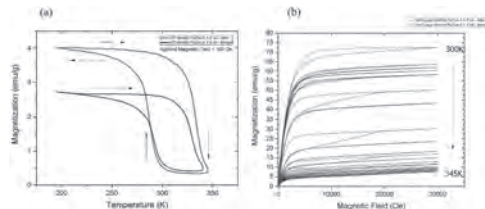


Fig.1 (a)MT Data from temperature range 200K-350K at 100Oe. (b)MH Loops 300K-345K exhibiting irradiation-induced hysteresis.

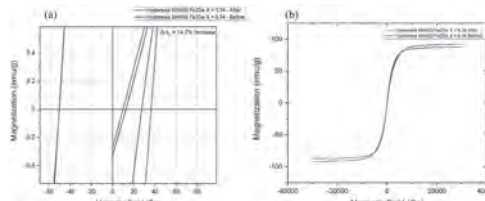


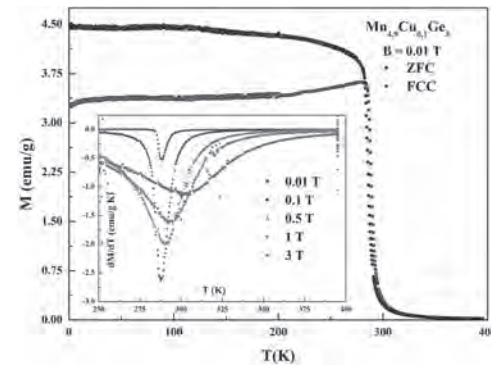
Fig.2 (a) Coercivity Data at 200K with an increase of 14.7% after treatment. (b) Hysteresis data from -3T to 3T at 200K.

**NPB-08. Near-room temperature magnetocaloric effect in Mn<sub>4.9</sub>Cu<sub>0.1</sub>Ge<sub>3</sub> compound.** S. Sakthivel<sup>1</sup>, A. Kumar<sup>1</sup>, U. Remya<sup>1</sup>, S. Athul<sup>1</sup>, A. Dzubinska<sup>2</sup>, M. Reiffers<sup>3</sup> and R. Nagalakshmi<sup>1</sup> 1. *Intermetallics and NLO Laboratory, Physics, National Institute of Technology Tiruchirappalli, Tiruchirappalli, India; 2. Center for Progressive Materials-Technology and Innovation Park, University Pavol Jozef Šafárik, Kosice, Slovakia; 3. Faculty of Humanities and Natural Sciences, Presov University, Presov, Slovakia*

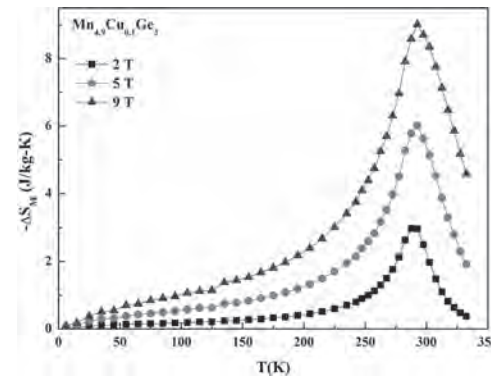
Magnetic refrigeration based on magnetocaloric effect is an effective technology to curb greenhouse gas emission. It is crucial to choose a viable magnetocaloric material with reversible room temperature magnetocaloric effect. Mn<sub>5</sub>Ge<sub>3</sub> based compounds are the perfect fit to this class. They are rare-earth free and exhibits a magnetic entropy change () of 9.3 J/kg K and relative cooling power () of 400 J/kg in = 5 T around 296 K<sup>1</sup>. Here, the magnetic interaction between and among the Mn atoms in 4d and 6g sites dictates the magnetocaloric effect which can be manipulated via tuning the Mn-Mn distance<sup>2</sup>. A best method to do so is doping and in this work, a non-magnetic element Cu is doped in place of Mn as a new attempt. Mn<sub>4.9</sub>Cu<sub>0.1</sub>Ge<sub>3</sub> polycrystalline compound, synthesized by arc melting method, has crystallized in Mn<sub>5</sub>Si<sub>3</sub>-type D8 hexagonal crystal structure (SG: P6<sub>3</sub>/mcm). The thermomagnetic measurements reveal a paramagnetic to ferromagnetic transition at 288.7 K, and shifts to higher value as the applied magnetic field is increased (Fig. 1). Arrott plot constructed from field-dependent magnetization demonstrates second order nature of the magnetic transition. In a magnetic field change of 5 T, Mn<sub>4.9</sub>Cu<sub>0.1</sub>Ge<sub>3</sub> compound shows = 6.03 J/kg K and RCP = 360.7 J/kg at 292 K (Fig. 2). The wide temperature working span has deemed its RCP closer to the parent compound and also it is comparable with other compounds in this class. The near-room temperature, second order

magnetocaloric effect are valuable properties for a magnetic refrigerator and this makes Mn<sub>4.9</sub>Cu<sub>0.1</sub>Ge<sub>3</sub> compound a remarkable magnetocaloric material. Acknowledgement: This work is the implementation of following projects and awards: DST-INSPIRE award (No. DST/INSPIRE/03/2018/000691), University Science Park TECHNICOM for Innovation Applications Supported by Knowledge Technology, ITMS: 26220220182, VEGA 1/0404/21 and VEGA 1/0705/20.

<sup>1</sup> T. Tolinski and K. Synoradzki, *Intermetallics* 47, 1 (2014). <sup>2</sup> Q. Zhang, J. Du, Y. B. Li, N. K. Sun, W. B. Cui, D. Li, and Z. D. Zhang, *J. Appl. Phys.* 101, 123911 (2007). <sup>3</sup> S. S. A. K. R. U. D. A. Dzubinska, M. Reiffers, and N. R. *Intermetallics* 132 (2021). <sup>4</sup> K. H. Kang, Y. Oh, J. H. Kim, E. J. Kim, H.-S. Kim, and C. S. Yoon, *J. Alloys Compd.* 681, 541 (2016). <sup>5</sup> K. H. Kang, J. H. Kim, Y. Oh, E. J. Kim, and C. S. Yoon, *J. Alloys Compd.* 696, 931 (2017).



Temperature dependent zero field cooled and field cooled curves in  $B = 0.01$  T. Inset:  $dM/dT$  vs  $T$  graph demonstrating shift in transition temperature in various magnetic fields



Magnetocaloric effect in Mn<sub>4.9</sub>Cu<sub>0.1</sub>Ge<sub>3</sub> compound

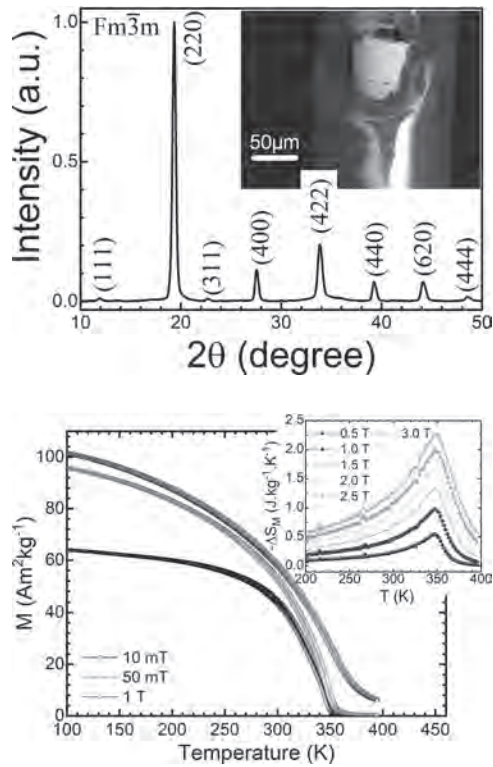
**NPB-09. Structural, magnetic and magnetocaloric characterization of Ni<sub>2</sub>MnSn microwires prepared by Taylor-Ulitovsky technique.**

*M.d. Arreguin Hernandez<sup>1,2</sup>, M. Varga<sup>1,3</sup>, M. Hennel<sup>1,3</sup>, T. Ryba<sup>4</sup>, J. Sanchez<sup>2,5</sup> and R. Varga<sup>3,4</sup> 1. Inst. Phys., Fac. Sci., UPJS, Kosice, Slovakia; 2. Materiales, IPICYT, San Luis Potosí, Mexico; 3. CPM-TIP, UPJS, Kosice, Slovakia; 4. RVmagnetic, Kosice, Slovakia; 5. Departamento de Física, Universidad de Oviedo, Oviedo, Spain*

In this work, we addressed the fabrication of Ni<sub>2</sub>MnSn glass-coated microwires (mws) by using the Taylor-Ulitovsky technique, as well as their structural, magnetic and magnetocaloric (MC) characterization. Apart from the physical characteristics of the material itself, wire-shaped MC materials bring additional features of interest from the viewpoint of refrigeration applications such as an easier magnetization saturation along wire length, and a large surface-to-volume ratio [1]. The former may lead to reach a given MC effect value at a lower magnetic field change  $m_0\Delta H$ , whereas the latter allows a high heat-transfer rate with the exchange fluid. Microwires were prepared from a bulk arc-melted ingot of nominal composition Ni<sub>2</sub>MnSn

produced from highly pure elements ( $\geq 99.9\%$ ). Their average metallic core diameter was  $86\text{ }\mu\text{m}$  (as the inset of Fig. 1(a) shows). Their characteristic XRD pattern, shown in Fig. 1(a), was indexed based on a single-phase austenite with the  $L_{21}$  structure (space group  $Fm-3m$ ;  $a=5.98\text{ \AA}$ ). The foreground graph in Fig. 1(b) shows that the  $M(T)$  curves measured upon heating and cooling cycles under magnetic fields  $m_0H$  of  $10\text{ mT}$ ,  $50\text{ mT}$ , and  $1\text{ T}$  almost overlap; austenite shows a Curie temperature of  $350\text{ K}$ . The thermal dependencies of the magnetic entropy change  $-\Delta S_M(T)$  for different  $m_0\Delta H$  values are shown at the inset of the figure; the curves are broad reaching a  $|\Delta S_M|^{max}$  value of  $2.3\text{ Jkg}^{-1}\text{K}^{-1}$  at  $3.0\text{ T}$ . The results are compared with those previously reported for bulk and melt-spun ribbons of the same composition [2,3].

[1] J. Alam et al., *J. Magn. Magn. Mater.* 513, 167074 (2020). [2] M. Nazmunnahar et al., *J. Magn. Magn. Mater.* 386, 98–101 (2015). [3] T. Krenke et al., *Phys. Rev. B* 72, 014412 (2005).



**NPB-10. Investigation Of Structural And Magnetic Properties Of Nanocrystalline  $Pr_{0.57}Bi_{0.1}Ca_{0.33}MnO_3$ .** G. Singh<sup>1</sup>, A. Gaur<sup>1</sup> and R.N. Mahato<sup>1</sup> *1. School Of Physical Sciences, JNU, New Delhi, India*

Perovskite manganite oxide shows that various future technologies (eg. spintronics, magnetic sensors, infrared detectors, magnetic storage media, colossal magneto-resistance application, thermo-electric applications, and magnetic refrigerants) are greatly relying on these materials [1]. Double exchange (DE) interaction and super-exchange (SE) interaction play a vital role in the above-given properties [2]. We have investigated the structural and magnetic properties of nanocrystalline powder  $Pr_{0.57}Bi_{0.1}Ca_{0.33}MnO_3$  (PBCMO) synthesized by the sol-gel technique. PBCMO is very interesting shows various magnetic transition as compare to  $La_{0.57}Bi_{0.1}Ca_{0.33}MnO_3$  which shows only one magnetic transition [3]. The Rietveld analysis of the X-ray diffraction (XRD) pattern reveals that the compound crystallizes in a single orthorhombic phase with the  $Pbnm$  space group. The Crystallite size was calculated using the Scherrer formula and it is found to be  $\sim 27\text{ nm}$ . Scanning electron microscope (SEM) images confirm the homogeneity of the sample and the average particle size from SEM image using particle size distribution with Lorentz fit was found to be  $110\text{ nm}$ . This has revealed that each particle consists of several crystallites. Temperature dependence Magnetization measurements under the external magnetic field

of  $500\text{ Oe}$ , in Fig.1, have shown that the sample exhibits magnetic transition at temperature  $\sim 44\text{ K}$  from ferromagnetic (FM) to paramagnetic (PM) phase with increasing temperature. Moreover, we have observed three small bumps near temperatures  $75\text{ K}$ ,  $158\text{ K}$ , and  $222\text{ K}$  that may suggest us simultaneous occurrence of the FM phase and antiferromagnetic phase [4]. Field-dependent magnetization for nanocrystalline PBCMO has exhibited ferromagnetism (FM) at low temperature ( $5\text{ K}$ ) and the linear hysteresis loop corresponds to the paramagnetic region at room temperature as shown in Fig.2.

1) Dipak Mazumdar, Kalipada Das and I. Das, *J. Appl. Phys.* 127, 093902-1 (2020) 2) A. Pal, A. Rao and D. Kekuda, *Journal of Magnetism and Magnetic Materials*. 512, 167011. 10.1016/j.jmmm.2020.167011. 3) Arpit Gaur, Meenakshi, Vipin Nagpal and Priyanka Bisht, *Solid State Communications*. 340, 114504. 10.1016/j.ssc.2021.114504. 4) J.R. Sun, J. Gao and Y. Fei, *PHYSICAL REVIEW B* 67, 144414 (2003)

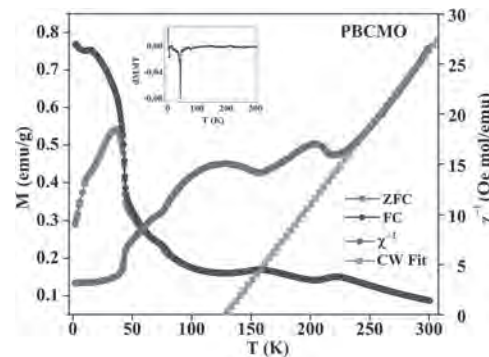


**Fig.1 Temperature dependence of FC and ZFC magnetizations for nanocrystalline  $Pr_{0.57}Bi_{0.1}Ca_{0.33}MnO_3$  sample at applied field of  $500\text{ Oe}$ .** Inset shows the derivative of  $M$  ( $T$ ) curve ( $dM/dT$  versus  $T$  plot).

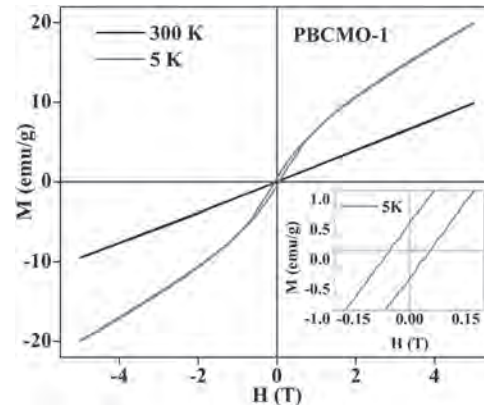


**Fig.2 Magnetisation ( $M$ ) versus applied magnetic field ( $H$ ) plot at  $5\text{ K}$  and  $300\text{ K}$  temperature.** Inset shows the magnified view of  $M$  versus  $H$  plot at  $5\text{ K}$ .

#### NPB-11. Withdrawn

**NPB-12. Magnetocaloric properties in  $Pr_xSr_xMnO_3(x=0.48$  and  $0.52$ ): Study using Landau and Maxwell Model.** A.K. Saw<sup>1</sup>, J.J. Nunez<sup>2</sup>, R.L. Hadimani<sup>2</sup> and V. Dayal<sup>1</sup> *1. Department of Physics, Maharaja Institute of Technology Mysore, Mandya, India; 2. Department of Mechanical and Nuclear Engineering, Virginia Commonwealth University, Richmond, VA, United States*

The magnetocaloric effect (MCE) is a common phenomenon in magnetic materials, and the essence of which is a thermal effect caused by the change of magnetic moment order under an adiabatic condition. A wide range of materials showing the first-order (FO)/second-order (SO) magnetic phase

Ravelosona, D. (COA-04).....	64	Riminucci, A. (MPA-10).....	413	Royer, F. (NOA-12).....	422
Ravelosona, D. (DOC-03).....	95	Rinaldi, C. (EOE-04).....	138	Rubano, A. (EOE-04).....	138
Ravelosona, D. (DOC-10).....	99	Rinaldi, C. (OOB-08).....	459	Rubini, G. (SC-04).....	12
Ravelosona, D. (HOA-05).....	243	Rinko, E. (JOA-06).....	304	Ruck, B. (COA-11).....	67
Ravelosona, D. (HOA-08).....	244	Rinko, E. (KOC-06).....	355	Ruck, B. (CPA-03).....	77
Ravelosona, D. (HOA-13).....	247	Riou, M. (DOC-03).....	95	Rucker, F. (EOC-07).....	128
Ravensburg, A.L. (LOA-09).....	384	Ripka, P. (OOB-06).....	458	Rudderham, C. (HOD-15).....	270
Ravi, S. (APA-02).....	37	Ritter, C. (AOB-09).....	30	Rueangnetr, N. (IOB-07).....	293
Ravi, S. (BPA-10).....	59	Ritter, C. (NOC-06).....	432	Ruffolo, L.J. (HPA-11).....	274
Ravi, S. (MPA-09).....	412	Rivas, M. (OOB-04).....	457	Ruhwedel, M. (EOC-11).....	129
Rawat, R. (BPA-01).....	55	Riveros, A. (HOA-04).....	242	Rui, X. (OOA-12).....	454
Ray, J. (ROB-07).....	543	Roberts, J.A. (NOA-07).....	420	Rui, X. (OOB-08).....	459
Reddy, V. (LOA-13).....	386	Robinson, J. (AOC-04).....	34	Ruijs, L. (MPA-11).....	413
Reddy, V. (MPA-02).....	410	Robinson, J. (DOA-03).....	81	Ruiz Gómez, S. (LOA-07).....	383
Reed, A. (BOA-11).....	48	Robinson, J. (FOD-11).....	192	Ruiz-Gómez, S. (EOC-01).....	126
Reese, B. (NPB-02).....	441	Robles-Kelly, C. (QPA-18).....	529	Ruiz-Gómez, S. (HOB-07).....	252
Reese, B.L. (MPA-08).....	412	Robles, R. (AOB-07).....	29	Ruiz-Gómez, S. (MOA-13).....	408
Rehm, L. (DOC-04).....	95	Rodolakis, F. (BOA-11).....	48	Rüßmann, P. (EOF-03).....	145
Reid, A.H. (GOA-09).....	203	Rodrigues, D.R. (EOC-13).....	130	Ryan, D. (KPC-05).....	372
Reid, A.H. (GOE-02).....	225	Rohart, S. (COB-02).....	68	Ryan, D. (NOC-06).....	432
Reid, A.H. (GOE-07).....	227	Rojas-Sánchez, J. (EOE-01).....	137	Ryapolov, P. (QPB-02).....	530
Reiffers, M. (NOC-03).....	431	Rojas, J. (NPB-07).....	443	Ryba, T. (NPB-09).....	444
Reiffers, M. (NPB-04).....	442	Romanova, A. (ROB-08).....	544	Ryou, H. (JOB-07).....	312
Reiffers, M. (NPB-08).....	444	Roos, M. (ROA-10).....	538	Ryu, J. (SG-05).....	23
Reig, C. (OPA-01).....	462	Rosch, A. (EOC-07).....	128	- S -	
Reimers, S. (EOA-10).....	114	Roschewsky, N. (EOF-02).....	145	S K, S. (HOD-09).....	268
Reith, H. (COA-05).....	64	Roschewsky, N. (EOF-11).....	149	S K, S. (HPA-20).....	278
Remya, U. (NOC-03).....	431	Rosenberg, E.R. (LOB-12).....	394	Sa, J. (QOB-05).....	516
Remya, U. (NPB-08).....	444	Ross, A. (SF-01).....	18	Sa, J. (QOB-06).....	516
Ren, H. (FOA-02).....	166	Ross, C.A. (BOA-04).....	45	Saavedra, E. (HOA-04).....	242
Ren, J. (PPB-05).....	488	Ross, C.A. (BOA-13).....	49	Saccione, M. (SC-03).....	12
Ren, P. (BOB-03).....	52	Ross, C.A. (FOA-06).....	168	Saccione, M. (SE-04).....	17
Ren, T. (HPA-17).....	276	Ross, C.A. (FOB-03).....	174	Saccione, M. (SE-05).....	17
Ren, Y. (COB-07).....	71	Ross, C.A. (GOD-04).....	220	Safonov, V. (NOA-07).....	420
Ren, Y. (ROB-04).....	541	Ross, C.A. (GOD-08).....	222	Safranski, C. (DOB-09).....	89
Ren, Y. (RPA-02).....	547	Ross, C.A. (JOB-03).....	311	Saglam, H. (EOA-05).....	111
Rennan Fu, R. (YA-01).....	3	Ross, C.A. (JPB-03).....	329	Saha, R. (GPA-05).....	233
Reshetniak, H. (GOB-08).....	209	Ross, C.A. (LOB-12).....	394	Saha, R. (QPA-06).....	523
Resnick, R. (EOB-07).....	121	Ross, C.A. (NPA-08).....	439	Saha, R. (RPA-04).....	548
Retterer, S.T. (LOA-05).....	382	Ross, J. (HPA-01).....	271	Saha, S. (GOA-02).....	201
Reuteler, J. (ROB-12).....	546	Rossel, M. (GOA-11).....	204	Saha, S. (GOD-02).....	219
Reyren, N. (DOC-10).....	99	Rostovtsev, Y.V. (NOA-07).....	420	Saha, S. (HPA-19).....	277
Reyren, N. (EOC-04).....	127	Rotarescu, C. (HPA-15).....	276	Sahin, C. (FOB-10).....	178
Reyren, N. (EOD-01).....	132	Rotarescu, C. (JPA-05).....	322	Sahu, B. (APA-08).....	39
Reyren, N. (EOE-08).....	140	Rotermund, F. (AOB-10).....	31	Sahu, P. (DOA-02).....	81
Reyren, N. (EOF-10).....	148	Rothörl, J. (DOC-09).....	98	Sahu, P. (SB-04).....	9
Reyren, N. (EPB-01).....	159	Rothörl, J. (HOD-10).....	268	Sahu, S. (FPA-15).....	200
Reyren, N. (FOB-02).....	173	Rothschild, A. (FOC-08).....	183	Sai, R. (JOA-03).....	303
Reyren, N. (HOD-03).....	265	Rothschild, A. (ROA-08).....	537	Sai, R. (JOA-07).....	305
Rhim, S.H. (EOE-10).....	141	Rougemaille, N. (SE-01).....	16	Sai, R. (JOA-08).....	305
Riah, Z. (OOB-09).....	460	Roussigné, Y. (COA-04).....	64	Sai, R. (OOB-03).....	457
Richardella, A. (FOB-10).....	178	Roussigné, Y. (HOA-08).....	244	Sait, C. (IOA-01).....	284
Richards, C. (ROB-07).....	543	Roussos, J.A. (NOA-06).....	419	Saito, M. (COC-05).....	73
Richter, C.A. (QPA-13).....	526	Rowan-Robinson, R. (JOC-03).....	317	Saito, S. (IPA-01).....	297
Richter, H. (DOB-05).....	87	Roy Chowdhury, R. (EOC-12).....	130	Saito, S. (IPA-03).....	298
Richter, K. (JPA-06).....	323	Roy, M. (NOC-11).....	435	Saito, T. (IPA-03).....	298
Rickhaus, P.S. (ROB-03).....	541	Roy, S. (COA-04).....	64	Saito, T. (KPA-13).....	362
Riegg, S. (NOA-02).....	416	Roy, S. (GOE-07).....	227	Saito, T. (KPC-04).....	371
Rieh, J. (SF-03).....	19	Roy, S. (HOA-05).....	243		
Riley, G. (DPA-04).....	103	Roy, S. (HOA-06).....	243		
Riminucci, A. (LOB-04).....	389	Roy, S. (HOB-11).....	254		

Saito, Y. (EOF-04) . . . . .	146	Sarkar, K. (NOC-11) . . . . .	435	Schneider, K. (JOA-10) . . . . .	306
Saito, Y. (FOB-06) . . . . .	175	Sarkar, R. (KOB-07) . . . . .	351	Schneider, M. (HOA-02) . . . . .	241
Saitoh, E. (EOB-02) . . . . .	118	Sarkar, T. (AOB-13) . . . . .	31	Schneider, M. (ROB-09) . . . . .	544
Saitoh, E. (GOA-06) . . . . .	202	Sarpi, B. (ROB-02) . . . . .	540	Schnitzspan, L. (EOB-02) . . . . .	118
Saitoh, E. (JOB-01) . . . . .	310	Sasaki, D.Y. (LOA-05) . . . . .	382	Schöbitz, M. (HOB-07) . . . . .	252
Sakai, T. (APA-14) . . . . .	41	Sasaki, J. (IOA-07) . . . . .	287	Schoeckel, A. (AOA-08) . . . . .	25
Sakakibara, R. (BOB-04) . . . . .	52	Sasaki, S. (PPC-12) . . . . .	503	Scholl, A. (AOB-04) . . . . .	28
Sakamoto, H. (QPA-01) . . . . .	520	Sasaki, S. (QPA-12) . . . . .	526	Scholl, A. (LOA-05) . . . . .	382
Sakamoto, M. (OOA-04) . . . . .	450	Sassi, A. (KOC-08) . . . . .	355	Scholz, M. (GOA-10) . . . . .	204
Sakamoto, M. (OOA-10) . . . . .	453	Sassi, Y. (DOC-10) . . . . .	99	Scholz, T. (EOF-03) . . . . .	145
Sakamoto, T. (QPA-11) . . . . .	525	Sassi, Y. (EOC-04) . . . . .	127	Schoop, L. (AOB-03) . . . . .	27
Sakthivel, S. (NOC-03) . . . . .	431	Sassi, Y. (EOD-01) . . . . .	132	Schrefl, T. (HOC-01) . . . . .	256
Sakthivel, S. (NPB-08) . . . . .	444	Sassi, Y. (EOE-08) . . . . .	140	Schrefl, T. (HOC-05) . . . . .	258
Sakuma, N. (HOC-01) . . . . .	256	Sassi, Y. (EPB-01) . . . . .	159	Schrefl, T. (HOC-11) . . . . .	261
Sakuma, N. (HOC-05) . . . . .	258	Sassi, Y. (FOB-02) . . . . .	173	Schrefl, T. (KOA-06) . . . . .	344
Sakuma, N. (KOA-06) . . . . .	344	Sassi, Y. (GOE-04) . . . . .	226	Schreiber, F. (EOB-02) . . . . .	118
Sakurai, H. (EOA-03) . . . . .	110	Sassi, Y. (HOD-03) . . . . .	265	Schuller, I.K. (EPA-04) . . . . .	153
Sala, G. (GOA-11) . . . . .	204	Sato, A. (QPA-01) . . . . .	520	Schuller, I.K. (EPA-08) . . . . .	155
Salaheldeen, M. (NOC-05) . . . . .	432	Sato, F. (PPC-12) . . . . .	503	Schultheiss, H. (GOC-12) . . . . .	216
Salahuddin, S. (DOB-12) . . . . .	91	Sato, F. (QPA-12) . . . . .	526	Schulz, F. (EOC-02) . . . . .	126
Salahuddin, S. (EOF-02) . . . . .	145	Sato, T. (JPC-06) . . . . .	337	Schulz, N. (CPA-01) . . . . .	77
Salahuddin, S. (EOF-11) . . . . .	149	Sato, Y. (EOB-04) . . . . .	119	Schumacher, H. (ROA-05) . . . . .	536
Salazar Carona, M.M. (HPA-06) . . . . .	272	Satz, A. (OOA-08) . . . . .	452	Schumacher, M. (GPA-13) . . . . .	237
Salazar-Mejia, J.M. (OOA-08) . . . . .	452	Saugar, E. (EOC-13) . . . . .	130	Schuman, C.D. (DOC-05) . . . . .	96
Salazar, D. (NOB-08) . . . . .	427	Saugar, E. (MOA-01) . . . . .	402	Schumann, T. (FOD-11) . . . . .	192
Saleheen, A.U. (HOB-11) . . . . .	254	Saugar, E. (ROA-05) . . . . .	536	Schütz, G. (EOC-02) . . . . .	126
Salimy, S. (ROA-06) . . . . .	537	Sauderson, T.G. (EOF-03) . . . . .	145	Schütz, G. (GOE-14) . . . . .	230
Sall, M. (HOA-08) . . . . .	244	Savadkoohi, M. (FOA-13) . . . . .	171	Schwartz, E. (EOF-06) . . . . .	147
Salomoni, D. (DPA-01) . . . . .	102	Savoyant, A. (BPA-15) . . . . .	60	Schwartz, E. (FOA-04) . . . . .	167
Salomoni, D. (GOA-07) . . . . .	203	Saw, A.K. (NPB-12) . . . . .	445	Schwartz, R.N. (DOA-10) . . . . .	84
Salomoni, D. (IOA-04) . . . . .	285	Sawano, K. (FOD-02) . . . . .	186	Scott, A. (QOA-16) . . . . .	513
Salter, W. (OPA-08) . . . . .	465	Sawano, K. (FOD-04) . . . . .	188	Scott, J. (LOB-01) . . . . .	388
Salvador, M. (OOB-04) . . . . .	457	Sayed, S. (DOB-12) . . . . .	91	Scott, J. (LOB-10) . . . . .	393
Samanta, A. (HOA-06) . . . . .	243	Sayed, S. (EOF-02) . . . . .	145	Scott, J.N. (IOA-01) . . . . .	284
Samarth, N. (DOA-02) . . . . .	81	Scagnoli, V. (GOA-10) . . . . .	204	Seema, S. (JOA-13) . . . . .	307
Samarth, N. (FOB-10) . . . . .	178	Scagnoli, V. (GOD-02) . . . . .	219	Seick, C. (GPA-13) . . . . .	237
Samartsev, A. (GOA-09) . . . . .	203	Scagnoli, V. (ROB-12) . . . . .	546	Seifert, T.S. (AOB-07) . . . . .	29
Samiepour, M. (IOA-09) . . . . .	288	Schaab, J. (EOC-01) . . . . .	126	Seki, T. (APA-10) . . . . .	39
Sampaio, J. (COB-02) . . . . .	68	Schäfer, L. (NOA-02) . . . . .	416	Seki, T. (EOB-05) . . . . .	120
Sampaio, J. (EOD-09) . . . . .	135	Schäfer, R. (ROB-11) . . . . .	545	Sekino, M. (QOA-15) . . . . .	512
<b>Sanchez Valdés, C.F. (NPB-04)</b> . . . . .	<b>442</b>	Schäfer, S. (ROB-06) . . . . .	543	Selsor, C. (KOC-07) . . . . .	355
Sanchez, J. (NPB-04) . . . . .	442	Scheibel, F. (NOA-02) . . . . .	416	Semenov, Y. (EOB-06) . . . . .	120
Sanchez, J. (NPB-09) . . . . .	444	Scheibel, F. (NOB-11) . . . . .	428	Seneor, P. (AOB-06) . . . . .	29
Sangaa, D. (MPA-14) . . . . .	414	Scheibel, F. (NOC-01) . . . . .	430	Seneor, P. (DOA-08) . . . . .	83
Sanger, Z. (QPA-06) . . . . .	523	Scherz, A. (GOA-09) . . . . .	203	Seneor, P. (DOC-10) . . . . .	99
Sanna, S. (LOB-04) . . . . .	389	Scheuerlein, M. (HOA-10) . . . . .	246	Seo, H. (EPB-08) . . . . .	162
Sano, T. (GPA-08) . . . . .	235	Schewe, J. (NPA-02) . . . . .	437	Seo, J. (AOC-08) . . . . .	35
Santos, E.J. (SA-02) . . . . .	5	Schewe, J. (QPB-05) . . . . .	532	Seo, J. (EOB-13) . . . . .	125
Santos, T. (DOB-05) . . . . .	87	Schiemenz, S. (COA-07) . . . . .	65	Seo, M. (GPA-03) . . . . .	233
Santos, T. (DOB-06) . . . . .	88	Schlappa, J. (GOA-09) . . . . .	203	Seo, Y. (EPA-06) . . . . .	154
Santos, T. (GOC-14) . . . . .	218	Schleife, A. (AOA-03) . . . . .	24	Seong, S. (EPA-06) . . . . .	154
Sanyal, B. (BOA-09) . . . . .	47	Schleife, A. (GOB-03) . . . . .	207	Sepehri-Amin, H. (IOB-02) . . . . .	290
Sanz Hernandez, D. (DOC-10) . . . . .	99	Schlitz, R. (AOB-07) . . . . .	29	Sepehri-Amin, H. (KOA-02) . . . . .	341
Sanz Hernandez, D. (DOC-12) . . . . .	100	Schluter, C. (LOA-13) . . . . .	386	Sepehri-Amin, H. (KOA-05) . . . . .	343
Sanz Hernandez, D. (GOE-04) . . . . .	226	Schmid, A. (SC-02) . . . . .	11	Sepehri-Amin, H. (NOB-02) . . . . .	424
Sanz Hernandez, D. (HOA-01) . . . . .	241	Schmidt, O.G. (ROB-11) . . . . .	545	Serdeha, I. (CPA-04) . . . . .	78
Sanz Hernandez, D. (SE-02) . . . . .	16	Schmitt, C. (EOB-02) . . . . .	118	Serdeha, I. (EOE-05) . . . . .	139
Sanz Hernandez, D. (SF-01) . . . . .	18	Schmitt, C. (GOA-06) . . . . .	202	Serpico, C. (GOC-05) . . . . .	213
Sanz-Hernández, D. (EOC-04) . . . . .	127	Schmitt, C. (OOA-08) . . . . .	452	Serpico, C. (GOD-07) . . . . .	222
Sapkota, A. (AOC-01) . . . . .	33	Schmitt, M. (EOF-03) . . . . .	145	Sethi, P. (DOC-12) . . . . .	100
Sarathlal, K. (LOA-13) . . . . .	386	Schneider, K. (JOA-09) . . . . .	306	Sethi, P. (GOE-04) . . . . .	226